J Food Sci Technol (March 2021) 58(3):1072–1080
https://doi.org/10.1007/s13197-020-04621-0

ORIGINAL ARTICLE

Evaluation of gas holes in "Queijo de Nisa" PDO cheese using computer vision

João Dias[1,2] · Patricia Lage[1] · Ana Garrido[3] · Eliana Machado[4] · Cristina Conceição[3,5] · Sandra Gomes[6] · António Martins[2,6] · Ana Paulino[7,8] · Maria F. Duarte[5,7] · Nuno Alvarenga[2,6]

Revised: 3 June 2020 / Accepted: 3 July 2020 / Published online: 11 July 2020

Abstract "Queijo de Nisa" is a traditional Portuguese cheese, granted with PDO label, produced with raw ewe's milk in which the aqueous extract of cardoon flower *Cynara cardunculus* L. is the only coagulant allowed. As in similar cheeses with no use of starter cultures or pasteurisation, the quality and food safety are depending on prevention, high hygienic standards and a proper manufacturing process. This study investigated the use of computer vision as novel method for the evaluation of gas holes in Queijo de Nisa in three different ripening dates (0, 15 and 35 days). A total of 48 samples were produced using cardoon flower from three different origins (C1, C2 and C3) and a commercial vegetable coagulant (C4). The results presented a high correlation between image-dependent attributes and physical–chemical properties during ripening time, especially within the first 15 days of ripening time, where major structural changes were observed inside the Queijo de Nisa cheese. Principal component analysis presented a strong correlation ($p < 0.05$) between image parameters and the physical–chemical evolution until 15 days. From 15 to 35 days, the evolution of cheeses was mainly depending on structural parameters, like $G'_{1\ Hz}$ and hardness. No influence was observed due to the geographical origin of cardoon flower.

Keywords Queijo de Nisa · PDO · Computer vision · Cardoon · Cheese

Introduction

In the last years, image analysis started to be used in different steps of the agro-food chain, for being objective, reliable, fast, and inexpensive (Donis-González and Guyer

✉ João Dias
joao.dias@ipbeja.pt

[1] Escola Superior Agrária, Instituto Politécnico de Beja, Rua Pedro Soares, Campus do Instituto Politécnico de Beja, 7800-295 Beja, Portugal

[2] Geobiosciences, Geobiotechnologies and Geoengineering (GeoBioTec), Faculdade de Ciências e Tecnologias, Universidade Nova de Lisboa, 2829-516 Caparica, Portugal

[3] Departamento de Zootecnia, Escola de Ciências e Tecnologia, Universidade de Évora, Pólo da Mitra, Ap. 94, 7006-554 Évora, Portugal

[4] Departamento de Biologia, Escola de Ciências e Tecnologia, Universidade de Évora, Pólo da Mitra, Ap. 94, 7006-554 Évora, Portugal

[5] MED – Mediterranean Institute for Agriculture, Environment and Development, Universidade de Évora, Pólo da Mitra, Ap. 94, 7006-554 Évora, Portugal

[6] Unidade de Tecnologia e Inovação, Instituto Nacional de Investigação Agrária e Veterinária, Avenida da República, Quinta do Marquês, 2780-157 Oeiras, Portugal

[7] Centro de Biotecnologia Agrícola e Agro-alimentar do Alentejo (CEBAL) / Instituto Politécnico de Beja (IP Beja), 7801-908 Beja, Portugal

[8] Centre for Ecology, Evolution and Environmental Changes (cE3c), Faculdade de Ciências, Universidade de Lisboa, 1749-016 Lisboa, Portugal

2016). The process of image analysis involves hardware and software. A digital camera can be used to capture the image, which is then analysed by image analysis software, able to perform various algorithms, such as colour space conversion and colour segmentation. Using these algorithms, the software is able to calculate colour information for each pixel on the entire sample surface (Cho et al. 2016). Additionally, the use of image analysis in the food industry has provided more accurate information than human vision, is more cost effective than a trained panel, no contact with sample is required, can provide information about the geometry of particles and may be integrated in automated inline inspections (Khattab et al. 2019).

Image analysis has been recently used in monitoring the browning of fruit (Cho et al. 2016), identification of defective hazelnuts (Giraudo et al. 2018), authentication of fish fillet (Grassi et al. 2018), estimation of berry ripening (Rodríguez-Pulido et al. 2012), counting of bacterial colonies (Chiang et al. 2015), among many others agro-industrial applications. Also, in cheese production, digital image analysis provides an efficient, and non-destructive tool that may complement human vision in the cheese analysis and sensorial quality evaluation, namely colour or cheese defects such as gas or mechanical holes, formation of calcium lactate crystals, excessive rind halo and oiling-off (Khattab et al. 2019). Actually, image analysis has been used successfully in Cheddar (Wang and Sun 2001), Mozzarella (Wang and Sun 2002), Parmigiano Reggiano (Iezzi et al. 2012) and Grana Padano cheeses (Iezzi et al. 2012).

In Portugal all traditional cheeses with Protected Designation of Origin (PDO) are made with raw milk, and therefore it is usual to find holes in these types of cheeses. "Queijo de Nisa" is a traditional Portuguese cheese produced with raw ewe's milk, granted with a PDO label (OJEC 1996), and characterized for a semi-hard consistency, with a white-yellow colour and sealed paste, with some small holes. "Queijo de Nisa" PDO cheese is manufactured in a limited geographic area of Portalegre district (south Portugal) using an aqueous infusion of *Cynara cardunculus* L (cardoon) dried flowers, as coagulant. The use of cardoon flowers as coagulant is a common practice in almost all ewe's milk PDO cheeses in Portugal (Gomes et al. 2019), but is also found in other ewe's cheeses from Spain, France or Italy (Fernández-Salguero and Sanjuán 1999), due to its alleged higher specificity for sheep milk (Conceição et al. 2018; Araújo-Rodrigues et al. 2020). However, these aqueous extracts are made actually from flowers of diverse *C. cardunculus* origins harvested at different flower development stages, influencing milk clotting activity and cheese properties (Ordiales et al. 2012). Although the presence of gas holes in raw milk cheese is natural and sometimes desirable, the PDO regulation of Queijo de Nisa cheese limits such holes to "some small holes" (DR 1993) showing, in some way, the decisive role of raw milk quality. Actually, there is not a specific limit value for the size, or percentage of gas holes, and is solely based on a conventional protocol, namely trained sensorial panel. The use of digital image could present itself as a reliable tool towards a standardization and monitoring of cheese quality, complementing sensorial evaluation, as a new objective method for visually detectable features.

The aim of this work was to develop a computer vision method to evaluate gas formation in Queijo de Nisa PDO cheese during ripening, testing batches produced with different origins of cardoon flower.

Material and methods

Cheesemaking and sampling

Four batches of ewe's milk cheese were manufactured in a cheese plant located in Monforte (Portugal) using different coagulants: C1 (cardoon flower collected in Herdade da Abóbada, Beja, Portugal), C2 (cardoon flower collected in Herdade do Peral, Évora, Portugal), C3 (cardoon flower collected in Herdade da Revilheira, Évora, Portugal) and C4 (commercial extract from cardoon flower, Abiasa, Spain). The milk was heated to 28 °C in an open steel vat. Later, salt (14 g/L) and *C. cardunculus* L. aqueous infusion (15 g cardoon flower/500 mL water) was added for the coagulation. After coagulation (at 32 to 37 °C for 60 min), the curd was cut and left for 15 min until the syneresis process was completed. The whey was drained and the curd was transferred to microperforated plastic moulds, previously lined with a cloth. The cheeses were pressed at 1.5 bar/20 min followed by 3.0 bar/25 min, in a pneumatic press, then the surface was rubbed with salt. The first stage of ripening was at 8–10 °C/80–90% relative humidity for 15 days (d). Later, cheeses were ripened at 10–12 °C/85–90% for 20 days. Four cheese samples were taken from each coagulant (C1, C2, C3 and C4) on each sampling date: 0, 15 and 35 days, transported and stored in a plastic bag at 4 °C for a maximum time period of 14 h.

Physical and chemical analysis

The moisture was performed according to ISO:5534/IDF:4 (2004) and the pH was evaluated with a penetration electrode at 20 ± 1 °C using a Metrohm 691 pH Meter (Herisau, Switzerland).

Rheological measurements were performed according to Alvarenga et al. (2011) at 20 ± 1 °C using a controlled shear-strain rheometer (Malvern Kinexus lab + , England)

connected to a refrigeration circuit with controlled temperature and a parallel plate geometry of 20 mm diameter, serrated in order to prevent slippage (Rosenberg et al. 1995) with 1 mm of gap distance. A strain sweep determination was performed on a different aliquot to ascertain linear viscoelastic (LVE) range. Finally, the mechanical spectrum (dynamic frequency sweep) was conducted applying a steady strain of 0.01%. All frequency sweeps were conducted with oscillation frequencies ranging from 0.001 to 100 Hz in three different samples (triplicate). The output of the rheometer measurements was the variation of storage modulus G′ (Pa) and the loss modulus G″ (Pa) as a function of the frequency f (Hz). The rheological parameter used in statistical treatments was storage modulus at 1 Hz ($G'_{1\ Hz}$, in Pa). A texture analyser TA.XT Plus100 (Stable Micro Systems, Godalming, UK), equipped with a 100 N load cell, was used to perform the texture analysis at 20 ± 1 °C. The procedure was implemented by puncture with a 10 mm diameter aluminium cylindrical probe, at a penetration depth of 20 mm (the height of the sample was 50 mm), with a crossed speed of 1 mm s^{-1}. Texture measurements were performed in triplicate: one in the core and the two others near the rind of the cheese. From the *force vs. time* texturograms, parameters "hardness" and "adhesiveness" were obtained, according to Alvarenga et al. (2008).

Image acquisition system

The digital image acquisition for each cheese was performed with a digital camera Canon M6, two D65 lamps and placing the sample over a black background (Fig. 1). A ruler was always included during image acquisition to set the scale, expressed in mm (Fig. 2). Images were acquired at a resolution of 6000 × 4000 pixel, 24 bits, sRGB, JPEG format, F/6.3, 1/40 seg, ISO100, no flash, and saved in uncompressed RAW format. A light unit with two fluorescent lamps with 11 W and 6500 K temperature was placed above cheese samples.

The image analysis was performed using ImageJ software version 1.52d (National Institute of Health, USA). The region of interest (ROI) of the image (Fig. 2) was selected, then the values of RGB components were obtained through the analysis of the histogram. Later, colour digital image (24-bit) was converted into grayscale (8-bit), then the segmentation of the holes was made adjusting threshold limits from 0 to 100 (Fig. 2). The following parameters were obtained after image analysis: number of holes, perimeter, Feret diameter (the maximum distance between any two points along the selection boundary) and minimum Feret (the minimum distance between any two points along the selection boundary). Shape factor (SF) was calculated according to Eq. 1 (Umesha et al. 2013).

$$SF = 4\pi \frac{Area}{Perimeter^2} \quad (1)$$

The area per hole and the percentage of the area occupied by gas holes was estimated based on the area of black holes and the total area of the slice of cheese, similar as Caccamo et al. (2004). The value of luminance (Y) was calculated according to Dias et al. (2016).

Statistical analysis

The average, standard deviation, and 0.95 confidence interval values were determined. Experimental data were subjected to One-way ANOVA (pairwise comparison of means with Scheffé test) in order to compare the average values of different samples. The multivariate exploratory techniques, a principal component analysis (PCA), was performed on the results to identify the key parameters describing a global data variability, and to monitor the ripening. Data were analysed using Statistica 6.0 (StatSoft, Tulsa, USA).

Results and discussion

Moisture content of cheese significantly decreased ($p < 0.05$) during ripening time (Table 1), caused by the natural and progressive loss of water (Delgado et al. 2009), to final values between 29,63% (35C4) and 35,70% (35C2).

The results are lower than in previous studies for PDO Nisa cheese (Freitas and Malcata 2000), where moisture presented values around 41%. The values of pH significantly decreased during ripening especially during the first 15 days, due to the production of lactic acid (Delgado et al. 2009) and confirming the predominance of lactic acid bacteria (Pinho et al. 2004). Similar results were obtained in La Serena (Del Pozo et al. 1988a), Torta del Casar (Delgado et al. 2009), Terrincho (Pinho et al. 2004) and Serpa (Alvarenga et al. 2008). Later, between 15 and 35 days, a slight increase of pH was observed, probably as a consequence of metabolic activity of micro-organisms which use lactic acid as a source of carbon and/or the proteolytic process that released alkaline nitrogenated compounds (Delgado et al. 2009). The obtained pH values, at 35 days, were similar to previous studies in Queijo de Nisa (Freitas and Malcata 2000) and Queijo Serpa (Santos et al. 2017).

The values of structural indicators, like storage modulus, adhesiveness and hardness, remained relatively stabilized from 0 to 15 days ($p > 0.05$), however, at 35 days an

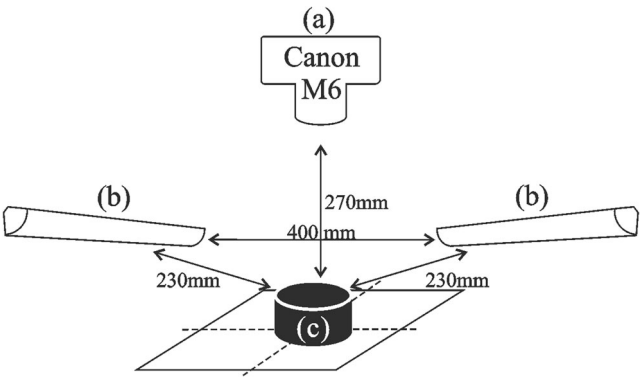

Fig. 1 Digital image analysis set up: **a** Camera, **b** fluorescent lamps with 11 W and 6500 K temperature **c** cheese sample

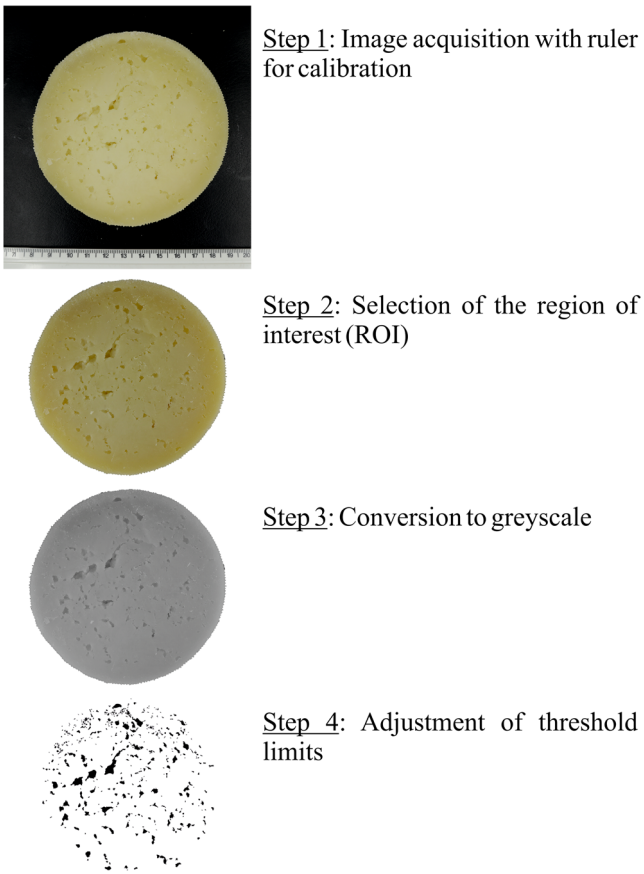

Fig. 2 Digital image processing, using 35d ripening time cheese as example

increase was observed ($p < 0.05$). Changes on structural parameters during ripening results on hardening, when the drying process has a dominant effect. On the other hand, the softness phenomenon is explained by prevalence of proteolysis of the α_{s1}-casein, usual in soft raw ewe's cheeses like Serpa (Alvarenga et al. 2008) or La Serena (Del Pozo et al. 1988b) cheeses. These opposite effects on the rheological properties of the cheese were explained by Gunasekaran and Ak (2003), on the basis of proteolysis reduces the storage modulus while drying has the opposite effect.

During the first 15 days of ripening time, a general increase was observed on R and G parameter of colour, followed by a decrease until the end of ripening time to minimum values (Table 1). Regarding B value, unlike R and G, this parameter decreased from the beginning till the end of ripening time (Table 1). The luminance (Y) of cheeses is calculated from RGB values, where higher values are related to white colour and lower values are related to black colour. At 0 day, luminance ranged between 174 and 177 and no significant differences ($p > 0.05$) were observed due to the origin of cardoon (C1 to C3) or vegetable rennet (C4). After 15 days, all samples

Table 1 Average values and standard deviation for physical, chemical and digital image parameters of the samples with 0, 15 and 35 days of ripening

	0 days				15 days				35 days			
	0C1	0C2	0C3	0C4	15C1	15C2	15C3	15C4	35C1	35C2	35C3	35C4
Moisture % (m/m)	59.13^{a}	60.33^{a}	57.55^{a}	49.40^{b}	41.45^{cd}	45.30^{bc}	40.15^{cde}	38.81^{c-f}	33.05^{efg}	35.70^{d-g}	32.21^{fg}	29.63^{g}
	(0.54)	(2.71)	(0.99)	(3.78)	(1.67)	0.36	(0.78)	(0.93)	(2.69)	(0.79)	(0.94)	(1.15)
pH	6.23^{a}	6.79^{a}	6.64^{a}	6.35^{a}	5.09^{b}	5.47^{b}	5.27^{b}	5.07^{b}	5.19^{b}	5.43^{b}	5.29^{b}	5.29^{b}
	(0.05)	(0.07)	(0.02)	(0.08)	(0.04)	(0.11)	(0.27)	(0.02)	(0.11)	(0.36)	(0.07)	(0.10)
$G'_{1\ Hz}$ (kPa)	73.0^{e}	108.9^{e}	131.4^{de}	150.4^{de}	40.3^{e}	172,6^{cde}	161.0^{de}	77.8^{e}	256.4^{bcd}	304.5^{bc}	444.6^{a}	316.2^{ab}
	(18.4)	(14.7)	(4.9)	(6.0)	(6.2)	(29.0)	(25.4)	(31.5)	(60.0)	(60.9)	(12.7)	(51.6)
Hardness (N)	13.99^{b}	24.47^{b}	24.58^{b}	28.26^{b}	28.68^{b}	46.77^{b}	53.5^{b}	49.61^{b}	165.86^{a}	136.63^{a}	173.34^{a}	153.18^{a}
	(1.19)	(6.92)	(2.49)	(1.16)	(3.74)	(4.34)	(6.90)	(5.46)	(10.60)	(9.53)	(29.32)	(10.58)
Adhesiveness (-N.s)	3.41^{b}	9.33^{b}	7.66^{b}	11.96^{b}	33.68^{b}	19.76^{b}	31.43^{b}	33.86^{b}	108.67^{a}	106.42^{a}	140.70^{a}	127.01^{a}
	(1.07)	(4.16)	(1.65)	(0.59)	(0.92)	(4.49)	(10.10)	(2.03)	(21.42)	(35.02)	(20.41)	(12.15)
R (−)	174.9^{b}	175.1^{b}	174.9^{b}	177.8^{b}	191.5^{a}	195.7^{a}	196.2^{a}	194.8^{a}	156.3^{c}	156.5^{c}	157.6^{c}	157.1^{c}
	(0.33)	(0.54)	(1.13)	(4.96)	(0.54)	(0.90)	(1.48)	(0.81)	(0.66)	(0.55)	(0.56)	(0.40)
G (−)	176.5^{c}	175.9^{c}	176.2^{c}	177.7^{c}	181.6^{bc}	191.9^{a}	190.4^{a}	183.9^{b}	145.3^{d}	148.0^{d}	149.6^{d}	146.5^{d}
	(0.34)	(0.40)	(1.33)	(2.37)	(0.51)	(1.73)	(3.45)	(1.16)	(0.91)	(0.70)	(0.48)	(0.54)
B (−)	168.3^{b}	165.7^{b}	166.8^{b}	171.4^{ab}	140.9^{d}	175.3^{a}	154.8^{c}	147.3^{d}	88.6^{f}	101.7^{e}	105.7^{e}	92.1^{f}
	(0.19)	(1.50)	(1.58)	(2.96)	(2.01)	(2.13)	(2.16)	(2.56)	(0.84)	(0.91)	(0.50)	(0.77)
Y (−)	175.1^{de}	174.5^{e}	174.7^{de}	177.0^{de}	180.0^{cd}	191.1^{a}	188.1^{ab}	183.0^{bc}	142.1^{f}	145.2^{f}	147.0^{f}	143.5^{f}
	(0.26)	(0.48)	(1.30)	(3.14)	(0.57)	(1.51)	(2.18)	(0.83)	(0.83)	(0.66)	(0.51)	(0.50)
Perimeter per hole (mm)	4.64^{c}	5.25^{bc}	7.51^{abc}	7.62^{abc}	8.06^{abc}	7.86^{abc}	7,66^{abc}	9.88^{ab}	5.92^{ab}	5.41^{b}	5.08^{b}	11.77^{a}
	(0.21)	(1.90)	(0.74)	(0.81)	(1.36)	(0.29)	(2.29)	(2.41)	(0.12)	(0.10)	(0.39)	(0.08)
Feret (mm)	1.52^{b}	1.70^{b}	2.38^{ab}	2.46^{ab}	2.24^{ab}	2.12^{ab}	2.37^{ab}	2.75^{ab}	1.81^{b}	1.78^{b}	1.65^{b}	3.28^{a}
	(0.02)	(0.50)	(0.23)	(0.30)	(0.32)	(0.04)	(0.62)	(0.81)	(0.10)	(0.06)	(0.08)	(0.10)
minFeret (mm)	0.84^{b}	0.97^{b}	1.29^{ab}	1.34^{ab}	1.27^{ab}	1.14^{ab}	1.41^{ab}	1.36^{ab}	1.01^{ab}	0.93^{ab}	0.93^{b}	1.87^{a}
	(0.01)	(0.27)	(0.08)	(0.18)	(0.22)	(0.06)	(0.45)	(0.47)	(0.05)	(0.01)	(0.07)	(0.05)
Shape factor (−)	0.50^{a}	0.52^{a}	0.45^{a}	0.48^{a}	0.42^{a}	0.37^{a}	0.42^{a}	0.51^{a}	0.44^{a}	0.48^{a}	0.50^{a}	0.39^{a}
	(0.04)	(0.09)	(0.02)	(0.04)	(0.04)	(0.01)	(0.06)	(0.06)	(0.02)	(0.01)	(0.03)	(0.01)
Percentage of holes (%)	1.41^{b}	0.97^{b}	0.53^{b}	1.12^{b}	7.34^{a}	7.20^{a}	7.46^{a}	6.59^{a}	6.20^{a}	3.98^{ab}	3.86^{ab}	6.60^{a}
	(0.10)	(0.24)	(0.08)	(0.35)	(2.00)	(0.87)	(0.93)	(2.05)	(0.94)	(0.09)	(0.56)	(0.94)
Area per hole (mm^2)	0.95^{b}	1.19^{b}	1.94^{b}	2.47^{b}	2.39^{b}	1.87^{b}	2.30^{b}	2.37^{b}	1.57^{b}	1.33^{b}	1.35^{b}	5.06^{a}
	(0.03)	(0.65)	(0.26)	(0.98)	(0.79)	(0.28)	(1.14)	(0.63)	(0.10)	(0.05)	(0.24)	(0.35)
Holes per unit area (holes cm^{-2})	1.14^{cd}	0.52^{d}	0.39^{d}	0.48^{d}	3.21^{abc}	3.96^{ab}	1.97^{bcd}	1.80^{bcd}	4.16^{a}	2.97^{abc}	2.80^{abc}	1.13^{cd}
	(0.61)	(0.13)	(0.26)	(0.19)	(0.84)	(0.17)	(0.85)	(0.51)	(0.75)	(0.23)	(0.72)	(0.36)

$^{a,b,c,\cdots}$ Means in the same row marked with different letters are significantly different ($p < 0.05$, n = 4, texture: Scheffé test)

presented a higher Y value, around 190, especially for C2 and C3 ($p < 0.05$). At 35 days, all samples presented darker appearance ($p < 0.05$), as stated by a significant lower value of Y, between 142 and 147. Similar results were observed other studies (Alvarenga et al. 2008; Lukinac et al. 2018).

Concerning perimeter, Feret diameter and minimum Feret, cardoons C1–C3 presented the highest values at 15 days, consistent with an increase of the dimensions of gas holes. Later, decreased until 35 days (Table 1) due to moisture loss and the consequent collapse of gas holes. On the other hand, coagulant C4, presented a continuous increase from 0 to 35 days (Table 1).

The evolution of cheese samples C2 and C4, during ripening, is presented in Fig. 3. At 0 day, both samples were similar, but at 15 days and 35 days different behaviours were noticed: (i) cheeses produced with C2 (also with C1 and C3, not shown) presented a normal gas formation for Queijo de Nisa PDO, according to DR (1993); (ii) cheeses produced with C4 presented abnormal gas holes and may not be suitable for Queijo de Nisa PDO. In Fig. 3 is also possible to observe that some holes presented

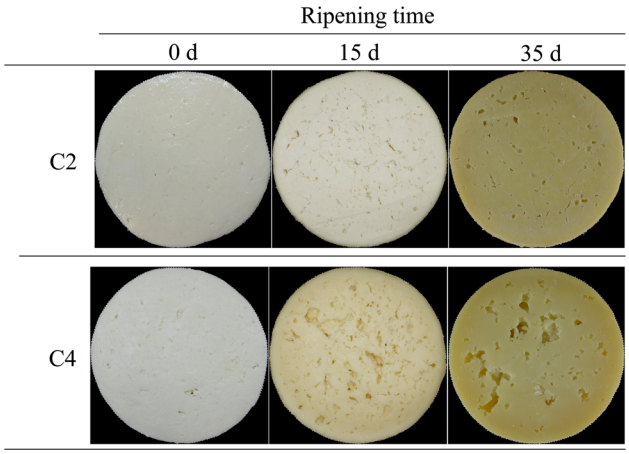

Fig. 3 Example images of samples during ripening time, produced with cardoon flower (C2) and vegetable coagulant (C4)

an irregular and angular shape, typical of mechanical holes (Caccamo et al. 2004).

The shape factor (SF) describes the degree of deformation and takes the value "1" for a perfect circle and close to "0" for a line (Umesha et al. 2013). The samples presented values between 0.37 and 0.52 (Table 1), not fully elongated nor fully circular. No influence was reported during ripening time or due to the coagulant ($p > 0.05$), revealing a steady structure.

The percentage of holes presented initial values around 0.53–1.41%, increasing to 6.59–7.46% at 15 days (Table 1). Later, cheeses produced with coagulants C2 and C3 decreased to 3.86–3.98%, until the end of ripening time. The highest value was observed in coagulant C4 at 35 days, around 6.60% (Table 1). Similar values were reported in studies on Ragusano cheese, where percentages between 0.93 and 6.84% were observed (Caccamo et al. 2004). According to literature, gas holes can be caused by coliform bacteria (Caccamo et al. 2004), yeasts, lactobacilli and may be an indicator of poor hygienic milk quality (Fox et al. 2017). Such species have been largely found in cheeses produced from raw ewe's milk in Spain and Portugal (Del Pozo et al. 1988b; Freitas and Malcata 2000). Also, yeasts have been profusely identified as natural flora of such artisanal cheeses such as Serpa cheese and have been identified as a major responsible for lactose fermentation (Santos et al. 2017).

The area per hole presented no significant differences ($p > 0.05$) during ripening (Table 1), excepting coagulant C4 increasing to 5.06 mm^2 at 35 days. The number of holes per unit area presented initial values around 0.39–1.14 holes cm^{-2}, increasing to 1.80–3.96 holes cm^{-2} at 15 days (Table 1), similar to previous studies on Cheddar cheese (Musse et al. 2014). At the end of ripening time, coagulant C1 presented the highest value (4.16 holes cm^{-2}) and C4 presented the lowest (1.13 holes cm^{-2}).

The Pearson's correlation coefficients (r) between image-dependent attributes and physical–chemical properties (Table 2), reinforced the importance of image analysis in this type of cheese. Strongly significant correlations were observed between the image parameters "percentage of holes"/"holes per unit area" and the physical–chemical parameters "pH"/"moisture"/"hardness". Other parameters, more dependent on the shape (like Feret and min-Feret), presented less significant correlations with the evolution of physical–chemical parameters (Table 2).

A PCA analysis was carried out on eleven parameters, namely colour (R, G, B and Y), morphological (percentage of holes, area per hole and SF), rheological ($G'_{1\ Hz}$ and hardness) and physical–chemical properties (moisture and pH). The similarity map defined by the first two principal components took into account 82.0% of the total variance (Fig. 4).

The first component (PC1) by itself condensed 54.8% and the second component (PC2) represented 27.2% of the total variance. The PC1 was explained by rheological parameters, moisture and colour and the PC2 was explained by pH, percentage of holes and area per hole. The PC1 presented negative correlations with $G'_{1\ Hz}$ and hardness and positive correlations with colour. The PC2 was negatively correlated to pH and positive correlated to percentage of holes and area per hole. Samples of cheeses during the first stage of ripening (between 0 and 15 days) progressed only in the PC2 from the negative to the positive region. It means that during this stage, the most important effect was pH, as in similar cheeses (Alvarenga et al. 2008), together with an increase in the size and area of the holes. Between 15 and 35 days, samples were separated mainly by CP1, from the positive to the negative region of this axis. However, CP2 also presented some influence because at 35 day samples were located in the centre of this axis. From 15 to 35 days ripening time it was possible to observe an increase on pH and on the structural parameters ($G'_{1\ Hz}$ and hardness) together with a decrease on moisture, percentage of holes and area per hole. Samples with same type of coagulant (C1–C4) are plotted together in the plan, which indicates a minor influence of the origin of coagulant. This effect can be observed in the distribution of samples in the plan in this analyse. However, in post-hoc Scheffé test the significant differences were observed in samples with different ripening time.

Conclusion

In Queijo de Nisa PDO cheese, the production of gas and consequently the arising of holes is normal to a certain extent (actually without any specific grade) and generally accepted by consumer. Although the regulation is not

Table 2 Pearson's correlation coefficients (r) between image-dependent attributes and physical–chemical properties

	pH	Moisture % (m/m)	G' 1 Hz (Pa)	Hardness (N)	Adhesiveness (-N.s)
Perimeter per hole (mm)	− 0.35*	− 0.32	− 0.07	0.01	0.05
Feret (mm)	− 0.24	− 0.27	− 0.06	− 0.01	0.04
minFeret (mm)	− 0.23	− 0.26	− 0.04	0.01	0.07
SF (−)	0.33*	0.27	− 0.07	− 0.07	− 0.09
Area per hole (mm^2)	− 0.42*	− 0.36*	− 0.07	0.05	0.12
Percentage of holes (%)	− 0.85**	− 0.67**	0.07	0.30	0.32
Holes per unit area (holes cm^{-2})	− 0.67**	− 0.55**	0.26	0.42**	0.40*

*Marked correlation significant ($0.01 < p < 0.05$)

**Marked correlation strongly significant ($p < 0.01$)

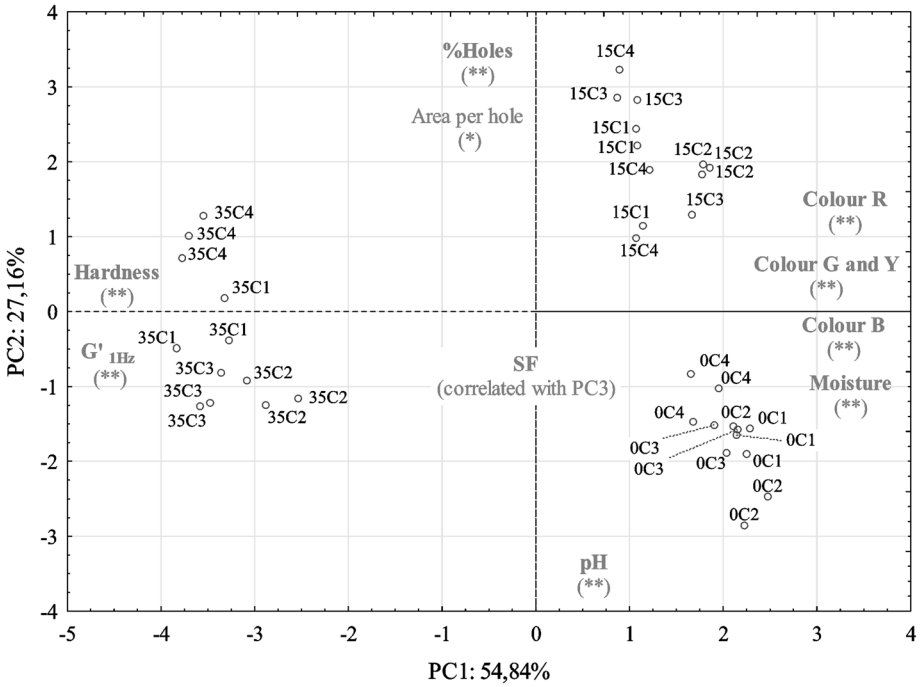

Fig. 4 Principal component analysis: PC1 vs. PC2 projection of samples (n = 3). The most important variables for the definition of the two components are shown on the edge of each axis, indicating the direction in which the value of the parameter increases. In the plot are represented samples produced with different coagulants (C1 to C4) with different ripening dates (0, 15 or 35 days). *Marked values were considered moderately correlated with the PC; **marked values were considered strongly correlated with the PC, following the classification used previously (Palma et al. 2009; Alvarenga et al. 2018)

detailed, excessive gas development is undesirable and may compromise PDO certification of such cheese. In this study, a novel methodology, based on computer vision, was developed for evaluating gas hole formation in Queijo de Nisa PDO cheese during ripening. This method provided a fast, simple and accurate approach providing a new insight for monitoring this type of traditional cheeses. It was found in this study that gas formation occurred mostly in the early 15 days of ripening time, presenting a significant development on perimeter, Feret diameter, minFeret and percentage of holes. A decrease in luminance was noticed in the later 20 days of ripening time. No influence was observed due to the geographical origin of cardoon flower, nevertheless the vegetable coagulant presented higher values for percentage, dimension and area per hole. This tool proved to be adequate, simple and objective to characterize cheeses where the presence of holes is common, although further quantitative aspects have to be found in accordance with other cheese quality parameters. Additionally, computer vision could also be extended to evaluate other visual features in PDO cheeses, like the evaluation of colour, however further studies are required for the definition of the appropriate lighting set.

Acknowledgements The authors thank to: (i) Regional Development European Foundation and Alentejo Region Program (ALENTEJO 2020) for their financial support to "ValBioTeCynara – Economic Valorisation of Cardoon (Cynara cardunculus): Study of natural variability and biotechnological applications" Project (ALT20-03-0145-FEDER-000038); (ii) National Funds through FCT—Foundation for Science and Technology for PhD grant to Ana Paulino (SFRH/BD/145383/2019), for project UIDB/05183/2020 and for

project UIDP/04035/2020; (iii) FEDER, through the Programa Operacional Regional de Lisboa and Programa Operacional Regional do Alentejo, and by national funds, through the Fundação para a Ciência e Tecnologia for their financial support to "CFD4CHEESE—Application of computational fluid mechanics in the optimization of ripening conditions of traditional cheeses" (ALT20-03-0145-FEDER-023356).

References

Alvarenga N, Silva P, Rodriguez Garcia J, Sousa I (2008) Estimation of Serpa cheese ripening time using multiple linear regression (MLR) considering rheological, physical and chemical data. J Dairy Res 75:233–239. https://doi.org/10.1017/S0022029908003191

Alvarenga N, Canada J, Sousa I (2011) Effect of freezing on the rheological and chemical properties of raw ewe's milk semisoft cheese. J Dairy Res 78:80–87. https://doi.org/10.1017/S0022029910000841

Alvarenga N, Taipina M, Raposo N, Dias J, Carvalho MJ, Amaral O, Santos MT, Silva MM, Lidon F (2018) Development of biscuits with green banana flour irradiated by ^{60}Co: preservation in modified atmosphere packaging. Emir J Food Agr 30:496–502. https://doi.org/10.9755/ejfa.2018.v30.i6.1720

Araújo-Rodrigues H, Tavaria FK, Santos MT, Alvarenga N, Pintado MM (2020) A review on microbiological and technological aspects of Serpa PDO cheese: an ovine raw milk cheese. Int Dairy J 100:104561. https://doi.org/10.1016/j.idairyj.2019.104561

Caccamo M, Melilli C, Barbano DM, Portelli G, Marino G, Licitra G (2004) Measurement of gas holes and mechanical openness in cheese by image analysis. J Dairy Sci 87:739–748. https://doi.org/10.3168/jds.S0022-0302(04)73217-8

Chiang PJ, Tseng MJ, He ZS, Li CH (2015) Automated counting of bacterial colonies by image analysis. J Microbiol Meth 108:74–82. https://doi.org/10.1016/j.mimet.2014.11.009

Cho JS, Lee HJ, Park JH, Sung JH, Choi JY, Moon KD (2016) Image analysis to evaluate the browning degree of banana (*Musa* spp.) peel. Food Chem 194:1028–1033. https://doi.org/10.1016/j.foodchem.2015.08.103

Conceição C, Martins P, Alvarenga N, Dias J, Lamy E, Garrido L, Gomes S, Freitas S, Belo A, Brás T, Paulino A, Duarte MF (2018) Chapter 5- Cynara cardunculus: use in cheesemaking and pharmaceutical applications. In: Koca N (ed) Technological approaches for novel applications in dairy processing. InTechOpen, London, pp 74–107

Delgado FJ, González-Crespo J, Ladero L, Cava R, Ramírez R (2009) Free fatty acids and oxidative changes of a Spanish soft cheese (PDO 'Torta del Casar') during ripening. Int J Food Sci Tech 44:1721–1728. https://doi.org/10.1111/j.1365-2621.2009.01987.x

Del Pozo B, Gaya P, Medina M, Rodríguez-Marín M, Nuñez M (1988a) Changes in the microflora of La Serena ewes' milk cheese. J Dairy Res 55:449–455. https://doi.org/10.1017/S0022029900028703

Del Pozo B, Gaya P, Medina M, Rodríguez-Marín M, Nuñez M (1988b) Changes in chemical and rheological characteristics of La Serena ewes' milk cheese during ripening. J Dairy Res 55:457–464. https://doi.org/10.1017/S0022029900028715

Dias JM, Almeida M, Adikevičius D, Andzevičius P, Alvarenga NB (2016) Impact of olive oil usage on physical properties of chocolate fillings. Grasas Aceites 67:e145. https://doi.org/10.3989/gya.0323161

DR (1993). Decreto Regulamentar N.° 6/93, on the delimitation of Demarcated Region for Queijo de Nisa cheese. Diário da República, Série B, N° 63 of 16th March, pp. 1239 (Portuguese Law)

Donis-González IR, Guyer DE (2016) Classification of processing asparagus sections using color images. Comput Electron Agr 127:236–241. https://doi.org/10.1016/j.compag.2016.06.018

Fernández-Salguero J, Sanjuán E (1999) Influence of vegetable and animal rennet on proteolysis during ripening in ewes' milk cheese. Food Chem 64:177–183. https://doi.org/10.1016/S0308-8146(98)00149-6

Fox P, Guinee T, Cogan M, McSweeney P (2017) Fundamentals of cheese science, 2nd edn. Springer, New York

Freitas C, Malcata F (2000) Microbiology and biochemistry of cheeses with Appélation d'Origine Protegée and manufactured in the Iberian Peninsula from Ovine and Caprine Milks. J Dairy Sci 83:584–602. https://doi.org/10.3168/jds.S0022-0302(00)74918-6

Giraudo A, Calvini R, Orlandi G, Ulrici A, Geobaldo F, Savorani F (2018) Development of an automated method for the identification of defective hazelnuts based on RGB image analysis and colourgrams. Food Control 94:233–240. https://doi.org/10.1016/j.foodcont.2018.07.018

Gomes S, Alvarenga N, Dias J, Lage P, Pinheiro C, Pinto-Cruz C, Brás T, Duarte M, Martins A (2019) Characterization of *Cynara cardunculus* L. flower from Alentejo as a coagulant agent for cheesemaking. Int Dairy J 91:178–184. https://doi.org/10.1016/j.idairyj.2018.09.010

Grassi S, Casiraghi E, Alamprese C (2018) Fish fillet authentication by image analysis. J Food Eng 234:16–23. https://doi.org/10.1016/j.jfoodeng.2018.04.012

Gunasekaran S, Ak MM (2003) Cheese rheology and texture, 1st edn. CRC Press, Boca Raton

Iezzi R, Locci F, Ghiglietti R, Belingheri C, Francolino S, Mucchetti G (2012) Parmigiano Reggiano and Grana Padano cheese curd grains size and distribution by image analysis. LWT Food Sci Technol 47:380–385. https://doi.org/10.1016/j.lwt.2012.01.035

ISO:5534/IDF:4 (2004) Cheese and processed cheese—determination of the total solids content (Reference method). International Organization for Standardization, Geneva, Switzerland

Khattab AR, Guirguis HA, Tawfik SM, Farag MA (2019) Cheese ripening: a review on modern technologies towards flavour enhancement, process acceleration and improved quality assessment. Trends Food Sci Tech 88:343–360. https://doi.org/10.1016/j.tifs.2019.03.009

Lukinac J, Jukić M, Mastanjević K, Lučan M (2018) Application of computer vision and image analysis method in cheese-quality evaluation: a review. Ukr Food J 192:192–214. 10.24263/2304-974X-2018-7-2-4

Musse M, Challois S, Huc D, Quellec S, Mariette F (2014) MRI method for investigation of eye growth in semi-hard cheese. J Food Eng 121:152–158. https://doi.org/10.1016/j.jfoodeng.2013.08.010

OJEC (1996). Commission Regulation (EC) No 1107/96 of 12 June 1996, on the registration of geographical indications and designations of origin under the procedure laid down in Article 17 of Council Regulation (EEC) No 2081/92. Official Journal of the European Communities No L 148.

Ordiales E, Martín A, Benito MJ, Hernández A, Ruiz-Moyano S, Córdoba MG (2012) Technological characterisation by free zone capillary electrophoresis (FCZE) of the vegetable rennet (*Cynara cardunculus*) used in ''Torta del Casar'' cheese-making. Food Chem 133:227–235. https://doi.org/10.1016/j.foodchem.2012.01.012

Palma P, Alvarenga P, Palma VL, Fernandes RM, Soares AMVM, Barbosa IR (2009) Assessment of anthropogenic sources of water pollution using multivariate statistical techniques: a case

study of the Alqueva's reservoir. Portugal Environ Monit Assess 165:539–552. https://doi.org/10.1007/s10661-009-0965-y

Pinho O, Mendes E, Alves MM, Ferreira IMPLVO (2004) Chemical, physical, and sensorial characteristics of "Terrincho" ewe cheese: changes during ripening and intravarietal comparison. J Dairy Sci 87:249–257. https://doi.org/10.3168/jds.S0022-0302(04)73163-X

Rodríguez-Pulido F, Gómez-Robledo L, Melgosa M, Gordillo B, González-Miret ML, Heredia FJ (2012) Ripeness estimation of grape berries and seeds by image analysis. Comput Electron Agr 82:128–133. https://doi.org/10.1016/j.compag.2012.01.004

Rosenberg M, Wang Z, Chuang S, Shoemaker C (1995) Viscoelastic property changes in Cheddar cheese during ripening. J Food Sci 60:640–644. https://doi.org/10.1111/j.1365-2621.1995.tb09846.x

Santos MT, Benito MJ, Córdoba MG, Alvarenga N, Herrera SRM (2017) Yeast community in traditional Portuguese Serpa cheese by culture-dependent and -independent DNA approaches. Int J Food Microbiol 262:63–70. https://doi.org/10.1016/j.ijfoodmicro.2017.09.013

Umesha SS, Monahar B, Naidu A (2013) Microencapsulation of a-linolenic acid-rich garden cress seed oil: physical characteristics and oxidative stability. Eur J Lipid Sci Tech 115:1474–1482. https://doi.org/10.1002/ejlt.201300181

Wang HH, Sun DW (2001) Evaluation of the functional properties of Cheddar Cheese using a computer vision method. J Food Eng 49:49–53. https://doi.org/10.1016/S0260-8774(00)00183-7

Wang HH, Sun DW (2002) Melting characteristics of cheese: analysis of effect of cheese dimensions using computer vision techniques. J Food Eng 52:279–284. https://doi.org/10.1016/S0260-8774(01)00116-9